Hindawi
International Journal of Polymer Science
Volume 2018, Article ID 7906208, 9 pages
https://doi.org/10.1155/2018/7906208

Research Article

Nano-Pr_2O_3 Doped PVA + $Na_3C_6H_5O_7$ Polymer Electrolyte Films for Electrochemical Cell Applications

J. Ramesh Babu,[1] **K. Ravindhranath**,[2] **and K. Vijaya Kumar**[1]

[1]*Department of Physics, K L University, Vaddeswaram, Guntur 522 502, India*
[2]*Department of Chemistry, K L University, Vaddeswaram, Guntur 522 502, India*

Correspondence should be addressed to J. Ramesh Babu; jallirameshura@gmail.com

Received 13 July 2017; Revised 9 October 2017; Accepted 18 October 2017; Published 2 January 2018

Academic Editor: Yulin Deng

Varying concentrations of nano-Pr_2O_3 doped in "PVA + Sodium Citrate (90 : 10)" polyelectrolyte films are synthesized using solution cast technique and the films are characterized adopting FTIR, XRD, SEM, and DSC methods. The film with 3.0% of nano-Pr_2O_3 content is more homogenous and possesses more amorphous region that facilitate the deeper penetration of nanoparticles into the film causing more interactions between the functional groups of the polymeric film and nano-Pr_2O_3 particles and thereby turning the film more friendlily to the proton conductivity. The conductivity is maximum of 7×10^{-4} S/cm at room temperature for 3.0% nano-Pr_2O_3 film and at that composition, the activation energy and crystallinity are low. With increase in temperature, the conductivity is increasing and it is attributed to the hopping of interchain and intrachain ion movements and furthermore decrease in microscopic viscosity of the films. The major charge carriers are ions and not electrons. These films are incorporated successfully as polyelectrolytes in electrochemical cells which are evaluated for their discharge characteristics. It is found that the discharge time is maximum of 140 hrs with open circuit voltage of 1.78 V for film containing 3% of nano-Pr_2O_3 and this reflects its adoptability in the solid-state battery applications.

1. Introduction

In view of easy mouldability, good contact with electrode materials, and less weight, the gel polymer electrolytes are assuming importance in electrochemical devices and in fact, they are intermediate between liquid electrolytes and solvent free ceramics [1, 2]. Many researchers developed polymer gel electrolytes with an aim to increase conductivity, durability, and film characteristics using host materials such as PMMA [3], PAN [4], PVdF [5], PEO [6], and PVA [7].

These polymeric electrolyte films suffer from exudation of liquid with time and get deteriorated. To prevent such ill-effects and to improve ionic mobility, inorganic electrolytes are incorporated in the films [8–11]. The literature survey indicates that PVA based gel electrolytes are increasingly been investigated as the host material because PVA is endowed with strong solvent affinity, good film formation, and good temperature window [12]. To increase the conductivity of films, proton materials such as acids like benzoic acid, dicarboxylic acids, phosphoric acid, and inorganic salts are used [13–15].

The most recent trend in this aspect of research work is to blend the films with nanomaterials of metal oxides in order to improve ionic conductivity, mechanical properties, and electrochemical stability for their adoptability in electrochemical devices [16]. The nanoparticles by virtue of size and large surface areas are endowed with dominant quantum characteristics besides the conventional properties they inherit due to their chemical compositions. This quantum nature has remarkable influence on catalytic, optical, electrical, and magnetic properties of the nanoparticles, resulting in their wide use in various industries, namely, nanoelectronics, clothing, sensors, cosmetics, tires, paints, and so on. The nanometal oxide when present in the films is remarkably influencing the film characteristics especially enhancing the conductivity of the films. Moreover, if the metal oxide is a rare oxide, the presence of many unpaired electrons present in the f-orbital of the metal ion may influence the magnetic

Table 1: DSC data pertaining to Tg, Mp, and % of crystallinity of PVA based films.

S number	Film composition-PVA + $Na_3C_6H_5O_7$ + nano-Pr_2O_3	Tg	Mp	% of crystallinity
(1)	Pure PVA	92.98	224.05	100
(2)	90 : 10 + 1%	91.11	222.44	80.25
(3)	90 : 10 + 2%	81.93	221.62	73.50
(4)	90 : 10 + 3%	75.27	220.74	65.34
(5)	90 : 10 + 4%	78.60	225.77	73.52

Table 2: Ionic conductivity, activation energy, and transference numbers of PVA + $Na_3C_6H_5O_7$ + nano-Pr_2O_3 polymer electrolyte films at different compositions.

Sl. number	Polymer electrolyte	Conductivity at 303 K (R_T) (S/cm)	Activation energy (E_a)	Transference number	
				t_{ion}	t_{ele}
(1)	Pure PVA	5.59×10^{-10}	0.42	—	—
(2)	PVA + $Na_3C_6H_5O_7$ + nano-Pr_2O_3 (90 : 10 : 1%)	3×10^{-4}	0.26	0.99	0.01
(3)	PVA + $Na_3C_6H_5O_7$ + nano-Pr_2O_3 (90 : 10 : 2%)	5×10^{-4}	0.24	0.96	0.04
(4)	PVA + $Na_3C_6H_5O_7$ + nano-Pr_2O_3 (90 : 10 : 3%)	7×10^{-4}	0.21	0.98	0.02
(5)	PVA + $Na_3C_6H_5O_7$ + nano-Pr_2O_3 (90 : 10 + 4%)	4×10^{-5}	0.39	0.95	0.05

and electric properties of the films by virtue of paramagnetic nature.

In our previous study on the binary blends of "Sodium Citrate in PVA + Sodium Citrate" films, we observed that the conductivity is more in the film containing 10% of Sodium Citrate [17].

Hence in this work, nanoparticles of a rare oxide Pr_2O_3 at various concentrations are blended with PVA (90%) + $Na_3C_6H_5O_7$ (10%) to obtain a composite film. Thus obtained film is characterized using XRD, SEM, DSC, FTIR, and AC impedance spectroscopy. The functionality of the film as solid gel electrolyte is assessed by fabricating an electrochemical cell with the developed film and investigating the various cell parameters.

2. Materials and Method

AR grade chemicals, namely, PVA (M.W. 85,000), Sodium Citrate, and Praseodymium Oxide, were used in this work. Triple distilled water was used in all the preparations. Praseodymium Oxide was milled for 8 hrs in Ball milling machine to 30–60 nm particles size and was used in this work.

The films were casted using solution casting technique [18]. Different proportions of PVA, $Na_3C_6H_5O_7$, and nano-Pr_2O_3 as detailed in Tables 1 and 2 were added to triple distilled water and stirred for 48 hours to get a homogeneous solution. Then the solution was poured in Petri dishes, dried at 40°C for 24 hrs, and then vacuum dried for 24 hrs. The dried films were peeled and characterized for XRD, SEM, FTIR, and DSC and their electrical properties were measured. Further, by using these films as solid polyelectrolyte, electrochemical cells were fabricated and their characteristics were assessed and presented in Table 4.

FTIR spectra were recorded using Perkin Elmer FTIR Spectrophotometer in range 4000 to 500 cm^{-1} adopting KBr pellet method with the resolution of 0.5 cm^{-1}. The spectra obtained were shown in Figure 1. XRD Bruker D8 instrument with Cu Kα radiation for 2θ angles between 10° and 60° (with scan rate: 2°/min and step size: 0.02°) was used to record spectra of the films and the obtained spectra was presented in Figure 2.

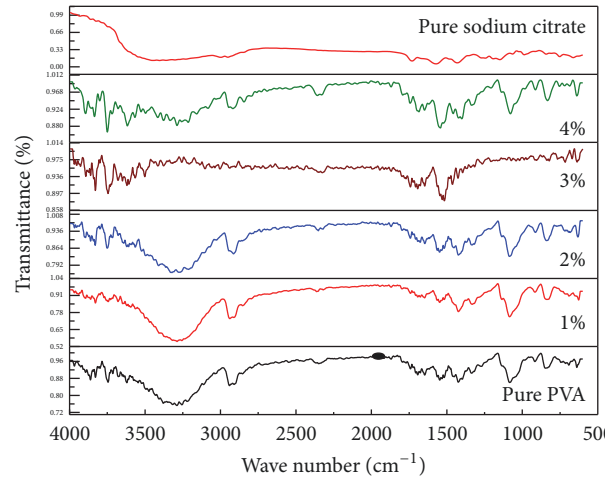

Figure 1: FTIR Spectra of polymeric films of compositions: PVA (90%) + Sodium Citrate (10%) + nano-Pr_2O_3 (1 to 4%) and Pure Sodium Citrate.

The Scanning Electron Microscope (SEM) images were recorded using FE-SEM, Carl Zeiss, and Ultra 55 model and presented in Figure 3.

Differential Scanning Calorimetry (DSC) thermograms were recorded using DSC Q20 V24.11 Build 124 (in N_2 atmosphere) for the composite films of PVA (90%) + $Na_3C_6H_5O_7$ (10%) + nano-Pr_2O_3 (1–4%) in determining the glass transition and melting temperatures and % of crystallinity. Three

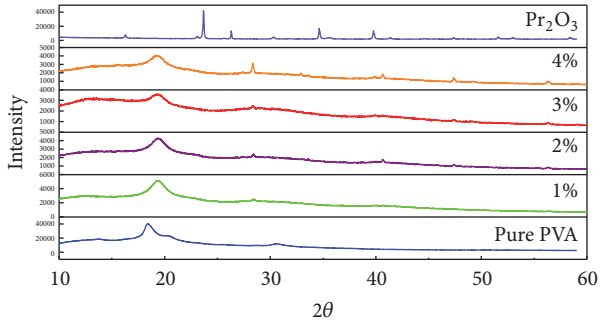

Figure 2: XRD Pattern of pure PVA and polymer electrolyte films of compositions: PVA (90%) + Sodium Citrate (10%) + nano-Pr_2O_3 (1 to 4%).

Table 3: Ionic conductivity values of PVA films at different temperatures.

S number	Composition of film: 90 : 10 + 3%	Conductivity S/cm
(1)	303 K	7×10^{-4}
(2)	313 K	8.2×10^{-4}
(3)	323 K	9.3×10^{-4}
(4)	333 K	1.1×10^{-3}

heating and cooling runs were performed and the averages of these values were presented in Figure 4 and Table 1.

The impedance measurements were carried out using a HIOKI3532-50 impedance analyzer in the frequency range from 50 Hz to 1 MHz at varying temperatures 303 K to 333 K. Measurements were performed thrice and their average is presented in the manuscript. The obtained results were presented in Tables 2 and 3 and Figures 5(a) and 5(b).

The transference number measurements were made using Wagner's polarization technique [19] and presented in Table 2 and Figure 6. Electrochemical cells were fabricated with the configuration of "Mg/$MgSO_4$ (anode)/polymer electrolyte/(I_2 + C + electrolyte) (cathode)." The discharge characteristics of the cell like open circuit voltage (OCV), short circuit current (SCC), power density, energy density, current capacity, and other parameters were measured under a constant load of 100 KΩ and the obtained values were presented in Figure 7 and Tables 4 and 5.

3. Results and Discussion

3.1. FTIR Analysis. FTIR spectra of the composite films of various compositions: PVA (90%) + Sodium Citrate (10%) + 1–4% of nano-Pr_2O_3, are depicted in Figure 1.

The pure PVA has broad peak in the range 3581–3055 cm^{-1} with centre at 3312 cm^{-1} pertains to -OH stretching. The broadness of the peak is attributed to the intra and/or intermolecular hydrogen bonding. But in the composite films, a drastic contrast is found in this peak as the % of nano-Pr_2O_3 is increased from 1.0% to 4.0%. The broad peak is shifted to 3435–3166 cm^{-1} with the centre at 3278 cm^{-1} for 1.0% of nano-Pr_2O_3; 3401–3155 cm^{-1} with centre 3445 cm^{-1} for 2.0% nano-Pr_2O_3 and sharp peaks appeared at 3547, 3502, 3413 cm^{-1} in 3.0% nano-Pr_2O_3 film. The decrease of broadening of the peaks along with shift towards lower wave number side as the % of nano-Pr_2O_3 is increased and further, the formation of sharp peaks when the % is 3, indicate the more homogenous mixing of the nano-Pr_2O_3 in the composite films.

The important peaks of Sodium Citrate component in the films are: 2880 and 2945 cm^{-1} for CH_2 stretching; 1466 and 1544 cm^{-1} for carboxylate ion; 1300 and 1070 cm^{-1} for C-O stretching; 3650, 3436, 3241 cm^{-1} for -OH stretching and 1625 cm^{-1} for -OHO bending.

The CH_2 frequency of pure PVA/PVA + $Na_3C_6H_5O_7$ at 2944 cm^{-1} is found to be shifted to lower wave side with decrease in intensity in composite films as the % of nano-Pr_2O_3 increases: with 1.0%, the shift is to 2909 cm^{-1}, with 2.0% the shift is to 2887 cm^{-1} and in 3.0% film, the peak is disappeared and further with 4.0%, the peak again appeared.

The stretching peak of Carbonyl group at 1745 cm^{-1} in pure PVA is shifted to 1723, 1700, 1686 1644 cm^{-1} as the % of nano-Pr_2O_3 is increased from 1.0 to 4.0%.

Further, the band pertaining to -C-O stretching at 1098 cm^{-1} in pure PVA/PVA + $Na_3C_6H_5O_7$ is shifted to 1062 cm^{-1}, 1051 cm^{-1}, and completely dispersed as the % of nano-Pr_2O_3 in the film is increased to 1.0%, 2.0% and 3.0% respectively. Again the peaks appeared at 1040 cm^{-1} when the % of nano-Pr_2O_3, is 4.0%. This indicates that the complete homogenous mixing of the nano-Pr_2O_3 in the film at 3.0% and it may be attributed to the formation of coordinating bond between the oxygen atom of PVA and Lewis acid nano-Pr_2O_3.

The variations in the position and nature of the frequencies of various functional groups namely, -OH, -O-, Carbonyl group, -CH_2, and so on reflect the complete and homogenous mixing of the components of the films especially when the film composition is: PVA (90%) + $Na_3C_6H_5O_7$ (10%) + nano-Pr_2O_3 (3%).

3.2. XRD. XRD data recorded for different composite of films were presented in Figure 2.

The well defined peaks in XRD spectra of Pr_2O_3 reflect the crystalline nature of the compound (Figure 2). Pure PVA has shown broad characteristic peak from 18 to 22°, in the 2θ range (110). With the addition of 10% of $Na_3C_6H_5O_7$ salt, the peak is broaden and sifted to 19.0° with decrease in intensity as we observed in previous work [20]. With the presence of nano-Pr_2O_3 in the film, the peak is shifted to 19.33° for 1.0%, 19.17° for 2.0%, 19.48° for 3.0% and 19.33° for 4.0% with increasing in broadening and decrease in intensity and it is interesting to note that at 3.0% the shift is maximum and well broaden with less intensity and without having characteristic sharp and strong peaks of Pr_2O_3 or $Na_3C_6H_5O_7$ or both. As is seen from the DSC data (Table 1), the crystallinity is found to be minimum at 3.0% of Pr_2O_3 indicating comparatively more amorphous regions at the said concentration. The amorphous nature allows the nanoparticles to penetrate deeper into the polymer matrix, thereby resulting in more innocuous interaction between the functional groups of the polymeric

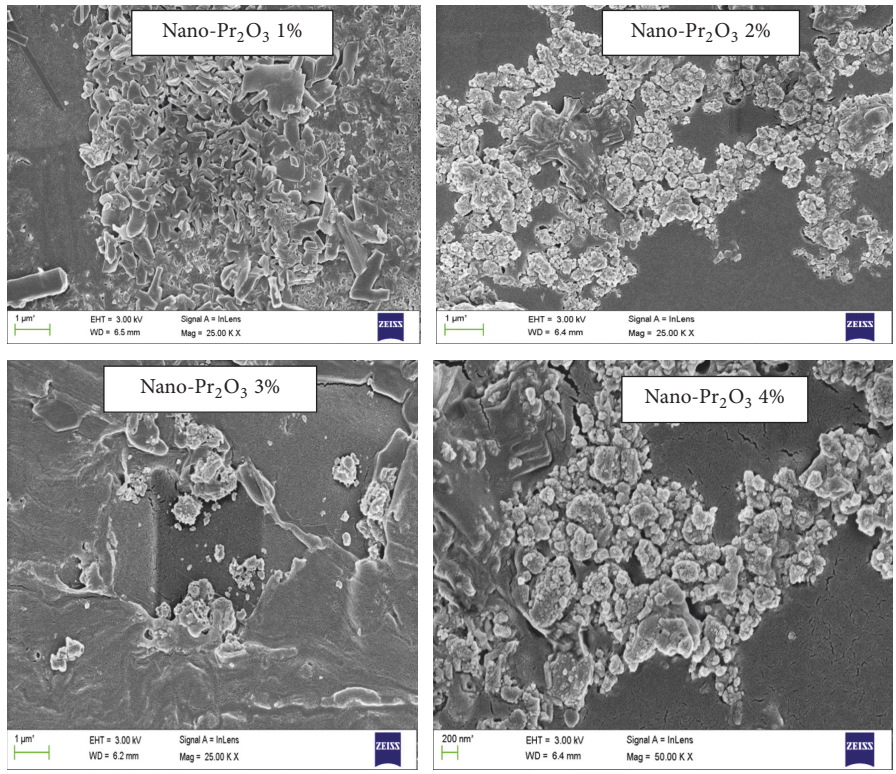

Figure 3: SEM images of composite films of PVA (90%) + $Na_3C_6H_5O_7$ (10%) + nano-Pr_2O_3 (1–4%).

Table 4: Cell parameters of PVA + Sodium Citrate + Pr_2O_3 at different compositions at constant load of 100 KΩ.

S number	Cell parameters	PVA + $Na_3C_6H_5O_7$ (90 : 10)	PVA + $Na_3C_6H_5O_7$ + Pr_2O_3 (90 : 10 : 1%)	PVA + $Na_3C_6H_5O_7$ + Pr_2O_3 (90 : 10 : 2%)	PVA + $Na_3C_6H_5O_7$ + Pr_2O_3 (90 : 10 : 3%)	PVA + $Na_3C_6H_5O_7$ + Pr_2O_3 (90 : 10 : 4%)
(1)	Open circuit voltage (V)	1.82	1.60	1.52	1.48	1.58
(2)	Short circuit current (μA)	0.26	0.56	0.48	0.34	0.46
(3)	Area of the cell (cm^2)	1.34	1.34	1.34	1.34	1.34
(4)	Weight of the cell (g)	1.40	1.40	1.40	1.40	1.40
(5)	Discharge time (h)	120	100	109	140	80
(6)	Power density (w/kg)	0.32	0.64	0.52	0.35	0.51
(7)	Energy density (wh/kg)	43.44	64	56.68	49	40.8
(8)	Current density ($\mu A/cm^2$)	196	417	358	253	343
(9)	Discharge capacity (mA-hr)	51.56	56	52.32	47.6	36.8

film and nano-Pr_2O_3 particles. These kinds of interactions result in complete dissolution of the ingredients in the film at the optimum 3% of nano-Pr_2O_3. But when the % of nano-Pr_2O_3 is increased more than 3.0%, again sharp peaks appeared indicating the precipitation of undissolved nano-Pr_2O_3 in the matrix of the film. Thus the composite films containing 3.0% of nano-Pr_2O_3 in PVA : $Na_3C_6H_5O_7$ (90 : 10), result in homogenous film.

3.3. SEM Analysis. The effects of increase of % composition of nano-Pr_2O_3 on the surface morphology of the composite

Table 5: Comparison of present cell parameters with the data of other cells reported earlier.

S. number	Solid state electrochemical cell configuration	Open circuit voltage (V)	Discharge time (hrs)	Reference number
(1)	$Ag/(PVP + AgNO_3)/(I_2 + C + electrolyte)$	0.46	82	[19]
(2)	$Ag/(PEO + AgNO_3)/(I_2 + C + electrolyte)$	0.61	48	[29]
(3)	$Na/(PEO + glass)/(I_2 + C + electrolyte)$	2.45	98	[30]
(4)	$Mg/PEO + Mg(NO_3)_2/(I_2 + C + electrolyte)$	1.85	142	[31]
(5)	$Na/(PVA + NaF)/(I_2 + C + electrolyte)$	2.53	122	[32]
(6)	$K/(PVP + PVA + KBrO_3)/(I_2 + C + electrolyte)$	2.30	72	[33]
(7)	$Mg/PVA + Mg(CH_3COO)_2/(I_2 + C + electrolyte)$	1.84	87	[34]
(8)	$K/(PEO + KYF_4)/(I_2 + C + electrolyte)$	2.40	51	[35]
(9)	$K/(PVP + PVA + KIO_3)/(I_2 + C + electrolyte)$ 45 : 45 : 10	2.50	160	[36]
(10)	$K/(PVP + PVA + KIO_3)/(I_2 + C + electrolyte)$ 40 : 40 : 20	2.60	168	[36]
(11)	$K/(PVP + PVA + KIO_3)/(I_2 + C + electrolyte)$ 35 : 35 : 30	2.70	176	[36]
(12)	$K/(PVP + PVA + KClO_3)/(I_2 + C + electrolyte)$	2.00	52	[36]
(13)	$Mg + MgSO_4/[PVA (90\%) + Na_3C_6H_5O_7 (10\%) + nano\text{-}Pr_2O_3(2\%)]/(I_2 + C + electrolyte)$	1.48	140	Present

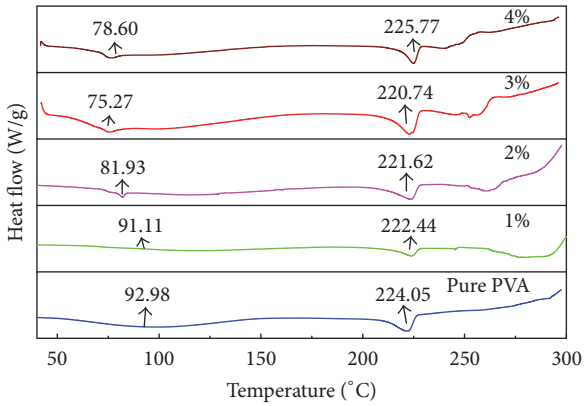

Figure 4: DSC curves of pure PVA and polymer electrolyte films of compositions: PVA (90%) + Sodium Citrate (10%) + nano-Pr_2O_3 (1 to 4%).

films: PVA (90%) + $Na_3C_6H_5O_7$ (10%) + nano-Pr_2O_3 (1–4%), are depicted in Figure 3.

It is seen from the images that the crystallinity is minimum when the % of nano-Pr_2O_3 is 3.0%. The observations are "in tandem" with the XRD data. The crystallinity loss of PVA films are attributed to the Lewis acid-base interactions at the interfaces of the nanoparticles with the PVA + Sodium Citrate. The increase in solubility and subsequent loss of crystallinity occur when the constituents of the film are closely related in chemical and physical characteristics. PVA, and Sodium Citrate and Pr_2O_3 have similarities in functional groups and more over Pr_2O_3 has Lewis acid nature. The Lewis nature of the metal ion in Pr_2O_3 evokes the "electron pair- donor" nature of the functional groups of PVA and Sodium Citrate such as C=O, =O and so on, resulting in the occupation of empty coordination sites of Pr by the functional groups of PVA and Sodium Citrate. Consequently, the nano-Pr_2O_3 shows more solubility in PVA + Sodium Citrate films. When the % of nano-Pr_2O_3 is 3.0%, it seems that the solubility reaches saturation point.

3.4. DSC Studies. DSC thermograms are recorded for pure PVA and PVA (90%) + $Na_3C_6H_5O_7$ (10%) + nano-Pr_2O_3 (1–4%) composite films and the obtained thermal scans are presented in Figure 4.

Glass transition temperature (Tg) and melting point (Mp) are found from the graphs. Further, % of crystallinities of the films are calculated using the equation [21] $\% \chi_c = \{(\Delta H_m)/(\Delta H_m{}^0)\} \times 100$, where $\Delta H_m{}^0$ is the melting enthalpy of $PVA : Na_3C_6H_5O_7$ (90 : 10) film and ΔH_m is melting enthalpy of related composite films containing nano-Pr_2O_3 at varied percentages. The Tg, Mp, and relative percentage of crystallinity (% χ_c) values are presented in Table 1.

It is seen from the table that the Tg and Mp values of PVA film are 92.98°C and 224.05°C, respectively. The presence of nano-Pr_2O_3 in the films has a marked effect on Tg, Mp, and crystallinity of films. With the composite films containing 1.0, 2.0, and 3.0% of Pr_2O_3, the Tg values decrease, respectively, to 91.11, 81.93, and 75.27°C; Mp values decrease to 222.44, 221.62, and 220.74°C; and % of crystallinity also decreases to 80.25, 73.50, and 65.34. The Tg, Mp, and crystallinity are the lowest when the composite films contain 3.0% of Pr_2O_3 and the film is more homogenous and plasticized and is accomplished with more amorphous nature. But with further increase of Pr_2O_3 to 4%, Tg, Mp, and % of crystallinity increase to 78.60°C, 225.77°C, and 73.52%, respectively. The nanoparticles of Pr_2O_3 enter between the crystalline chains of PVA and hold them firmly through the various functional groups, thereby resulting in the dissolution of the ingredients of the composite film. This is reflected in the fact that, as the % of nanoparticles increase, there is a decrease in crystallinity,

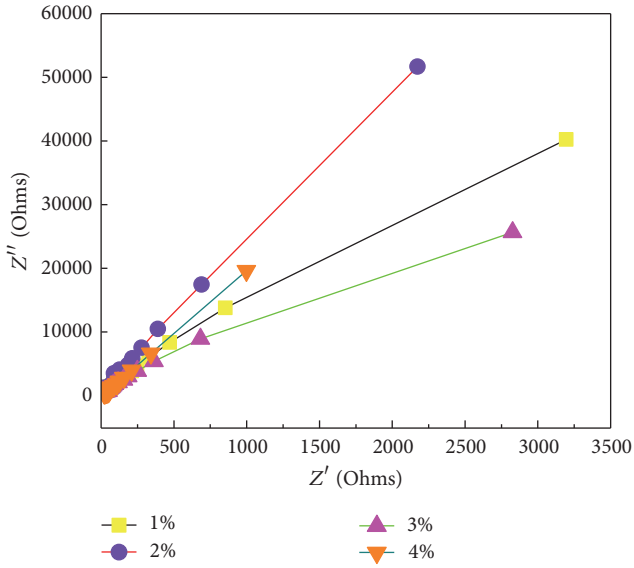

(a) Impedance plots of polymeric electrolyte films of compositions PVA (90%) + Sodium Citrate (10%) + nano-Pr_2O_3 (1 to 4%)

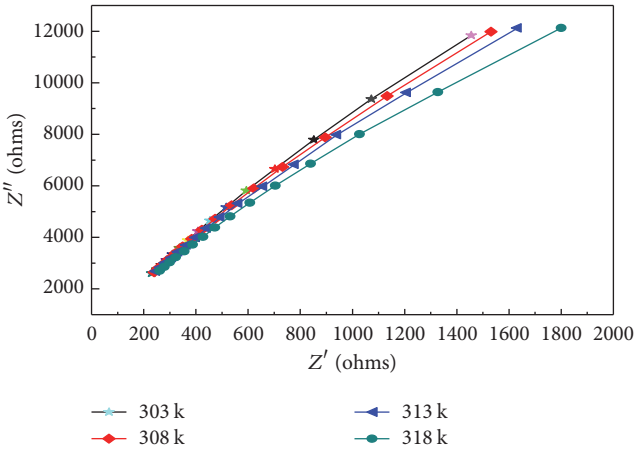

(b) Complex impedance at different temperatures of polymeric electrolyte films of compositions PVA (90%) + Sodium Citrate (10%) + nano-Pr_2O_3 (1 to 4%)

Figure 5

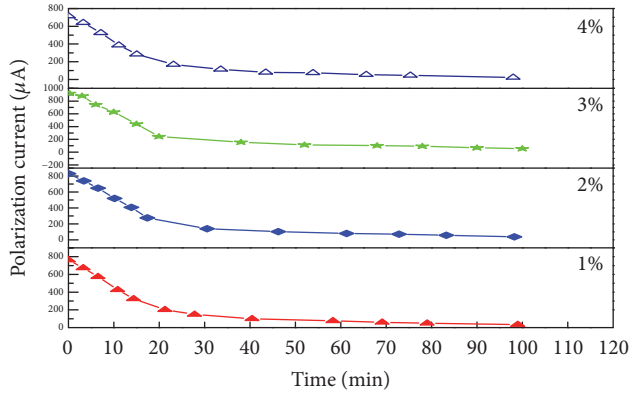

Figure 6: Transference number measurements for polymeric electrolyte films of compositions PVA (90%) + Sodium Citrate (10%) + nano-Pr_2O_3 (1 to 4%).

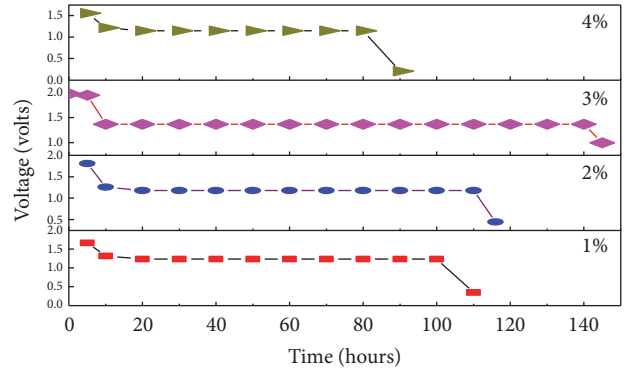

Figure 7: Discharge characteristics plots of PVA (90%) + $Na_3C_6H_5O_7$ (10%) + nano-Pr_2O_3 (1–4%). Electrochemical cell for constant load of 100 KΩ.

Tg, and Mp values. This effect is found to reach maximum when the % of Pr_2O_3 is 3%. On further increase of the nanoparticles percentage, the crystallinity, Tg, and Mp are found to be increasing as the film is deemed to reach its saturation value with respect to nano-Pr_2O_3 at 3.0% and any further addition result in the precipitation of the nano-Pr_2O_3 on to the polymeric chains as unabsorbed crystals. Thus the composite film containing 3.0% of Pr_2O_3 has less crystallinity and is more homogeneous and so it is viable to more proton conductivity.

3.5. Impedance Analysis. The complex impedance (CI) plots of the different films were drawn by measuring the conductivity using HIOKI3532-50 impedance analyzer at temperature 303 K. The measurement were noted by sandwiching PVA : $Na_3C_6H_5O_7$: nano-Pr_2O_3 films between thin stainless steel plates The conductivity was calculated using the formula: $\sigma = l = R_b/A$ in S/cm, where σ is ionic conductivity, l is thickness of the polymer electrolyte film, R_b is bulk resistance, and A is area of the stainless steel electrode contacting the polymer electrolyte film. The measurements were made at room temperature for the films containing varying % of nano-Pr_2O_3 and by varying the temperature for a film containing optimum amount of Pr_2O_3, that is, 3.0% (which was showing higher conductivity). The observations were presented in Figures 5(a) and 5(b) and Table 2.

The major contributors for the conductivity are the ions. It is seen from the data that the conductivity increases with the increase in nano-Pr_2O_3 content but it is not linear. It reaches a maximum value at 3 wt.% of nano-Pr_2O_3 and it decreases when the % of nano-Pr_2O_3 is increased further to 4 wt.%. The presence of nano-Pr_2O_3 modifies the structure of the composite film by virtue of its high surface area, quantum confinements, and further cross-lining of PVA + $Na_3C_6H_5O_7$ segments. Such modifications generate additional pathways in the film that complements the ionic movement [22–24].

At low Pr_2O_3 percentages, the dissociation of $Na_3C_6H_5O_7$ is more and further it is inferred from the XRD data that the amorphous region is also more. This causes free movement of ions through the pathways in the amorphous region resulting

in the enhancement of conductivity. The optimum concentration of Pr_2O_3 is found to be 3.0%. Above this percentage, the nano-Pr_2O_3 seems to agglomerate and block some of the path ways for the movement of ions causing the decrease in conductivity. Moreover, the decrease in conductivity at higher % of nanoparticles may also be contributed because of the increase in microscopic viscosity of the film composite due to the presence of higher amounts of nano-Pr_2O_3.

Further, it is noted from Figure 5(b) and Table 3 that, as the temperature increases, the conductivity is found to be increasing. It may be due to the hopping of interchain and intrachain ion movements and decrease in viscosity of the composite film.

3.6. Transference Numbers. For the classification of polymer electrolyte films, ionic transference number is considered to be one of the most significant parameters. By using Wagner's polarizing technique, the transference numbers for the films were measured by constructing a system of Mg/(PVA + $Na_3C_6H_5O_7$ + Pr_2O_3)/C (sandwiched between two thin stainless steel plates) and polarizing it at 303 K at a constant dc potential of 1.5 V in order to assess the contributions of ions and electrons to the entire conductivity of the polymer electrolyte films. The equations used are

$$t_{\text{ion}} = \frac{I_{\text{initial}} - I_{\text{final}}}{I_{\text{initial}}} = \frac{I_{\text{total}} - I_{\text{electronic}}}{I_{\text{total}}} = \frac{I_{\text{ionic}}}{I_{\text{total}}}, \quad (1)$$

where I_{initial} is the initial current and I_{final} is the final current. The ionic transference number (t_{ion}) values are in the range of 0.99–0.95. The results were presented in Figure 6 and Table 2.

It can be inferred from Table 2 that the charge carriers are predominantly ions and not electrons in all the composite films. The ionic conductivity is found to be high in the films containing the optimum 3.0 percentage of Pr_2O_3 at which the activation energy and crystallinity are low. Further, the ionic transference number (t_{ion}) of the films is near to unity indicating its suitability as a polymer electrolyte for solid-state electrochemical cells [25–27].

3.7. Discharge Studies. Discharge studies were made by fabricating solid-state electrochemical cells using the present developed poly electrolyte films (containing the varying percentages of nano-Pr_2O_3) in the configuration: anode (Mg + $MgSO_4$)/[PVA (90%) + $Na_3C_6H_5O_7$ (10%) + nano-Pr_2O_3 (1–4%)]/cathode (I_2 + C + electrolyte) under a constant load of 100 kΩ at room temperature. The anode pellet was made of Mg + $MgSO_4$ while the cathode pellet was made of "I + C + polymer electrolyte." The presence of carbon in the cathode increases the conductivity and poly electrolyte reduces the resistance by allowing the more interfacial contact between the cathode and electrolyte [28]. The thickness of both the electrodes was 1 mm while the surface area and thicknesses of the PVA + $Na_3C_6H_5O_7$ + nano-Pr_2O_3 electrolyte were 1.34 cm^2 and 150 μm, respectively.

Various parameters such as open circuit voltage (OCV), short circuit current (SCC), current density, power density, energy density, discharge time, and discharge capacity were evaluated for all the systems. The obtained values were presented in Table 4 and Figure 7.

It is seen from the data that the discharge time is maximum with a value of 140 hrs with the films containing 3.0% of nano-Pr_2O_3 indicating the successful adoption of the polyelectrolyte films (at the said composition) in the battery applications.

4. Comparison with Previous Work

The present developed electrochemical cell is compared with hitherto reported cells in the literature and the comparative assessment is presented in Table 5.

From these cell parameters, it is clear that the present electrolyte system is more efficient than many of the reported cells in the literature. Hence, it may be concluded that the developed solid-state electrochemical cell is simple, efficient, reliable, and having long discharge times besides being economical and environment friendly. This developed electrochemical cell may find its applications as cost effective electrolyte in high density solid-state electrochemical cells.

5. Conclusions

Good polyelectrolyte films of PVA + Sodium Citrate (90 : 10) containing varied amounts of (1–4%) of nano-Pr_2O_3 are synthesized using solution cast technique. The films are characterized to understand their physicochemical nature by adopting FTIR XRD and SEM techniques. The variations in the positions and nature of the frequencies of various functional groups in the FTIR spectral features of the films and further the SEM studies reveal that the different components of the films are completely and homogenously mixed. At 3.0% of nano-Pr_2O_3, the dispersion of the later in the film is more thorough and uniform. XRD pattern of the films also reveals the same. At 3.0%, the crystallinity is low indicating more amorphous nature of the film. The amorphousness regions of the film are conductive for the nanoparticles to penetrate deeper into the polymer matrix and this results in more interactions between the functional groups of the polymeric film and nano-Pr_2O_3 particles, thereby imparting more homogenous nature of the film. DSC studies also reveal that, with the composite films containing 3.0% of Pr_2O_3, the amorphousness is more and this nature is friendlier to proton conductivity.

The conductivity of synthesized composite films is increasing with increase of % of Pr_2O_3 and is maximum at 3.0% of Pr_2O_3 and on further increase, the conductivity decreases indicating the saturation of the film with the nano-Pr_2O_3. The conductivity is found to be 3×10^{-4}, 5×10^{-4}, 7×10^{-4}, and 4×10^{-5} S/cm at 1.0%, 2.0%, 3.0%, and 4.0% of Pr_2O_3, respectively. Further, as the temperature increases, the conductivity is increasing and it is attributed to the hopping of interchain and intrachain ion movements and decrease in microscopic viscosity of the film. The activation energy and crystallinity are low with the films containing 3.0% of Pr_2O_3 resulting more conductivity. Transference numbers data reveal that the charge carriers are predominantly "ions"

and not "electrons." These polyelectrolyte films at various compositions of nano-Pr_2O_3, are incorporated in the configuration of electrochemical cells: "anode (Mg + $MgSO_4$)/[PVA (90%) + $Na_3C_6H_5O_7$ (10%) + nano-Pr_2O_3 (1–4%)]/cathode (I_2 + C + electrolyte)," and their discharge characteristics are evaluated. With 3% of nano-Pr_2O_3 films, the discharge time is maximum of 140 hrs with open circuit voltage of 1.78 V reflecting the successful adoption of the said composite film in the solid-state battery applications.

Conflicts of Interest

The authors declare that there are no conflicts of interest regarding the publication of this paper.

Authors' Contributions

The authors attest to the fact that all authors listed on the title page have contributed significantly to the work, attest to the validity and legitimacy of the data and its interpretation, and agree to its submission.

Acknowledgments

The authors acknowledge K L University authorities for providing the necessary facilities and financial help to carry out this research work.

References

[1] J. R. MacCallum and C. A. Vincent, *Polymer electrolyte reviews*, J. R. MacCallum and C. A. Vincent, Eds., Elsevier Applied Sciences Publisher, London, UK, 1989.

[2] B. Scrosati and C. A. Vincent, "Polymer electrolytes: The key to lithium polymer batteries," *MRS Bulletin*, vol. 25, no. 3, pp. 28–30, 2000.

[3] O. Bohnke, C. Rousselot, P. A. Gillet, and C. Truche, "Gel Electrolyte for Solid-State Electrochromic Cell," *Journal of The Electrochemical Society*, vol. 139, no. 7, pp. 1862–1865, 1992.

[4] F. Groce, F. Gerace, G. Dautzemberg, S. Passerini, G. B. Appetecchi, and B. Scrosati, "Synthesis and characterization of highly conducting gel electrolytes," *Electrochimica Acta*, vol. 39, no. 14, pp. 2187–2194, 1994.

[5] J. Y. Song, Y. Y. Wang, and C. C. Wan, "Conductivity study of porous plasticized polymer electrolytes based on poly(vinylidene fluoride). A comparison with polypropylene separators," *Journal of The Electrochemical Society*, vol. 147, no. 9, pp. 3219–3225, 2000.

[6] D. Radhucha, W. Wieczorek, Z. Florjanczyk, and J. Stevens R, "Nanaqueous H_3PO_4-doped gel electrolytes," *The Journal of Physical Chemistry A*, vol. 100, p. 6, 2012.

[7] F. Cavalieri, E. Chiessi, C. Spagnoti, and M. Cowman K, "Poly(vinyl alcohol) as versatile biomaterial for potential biomedical applications," *Journal of Materials Science: Materials in Medicine*, p. 14687, 2003.

[8] I. Honma, S. Hirakawa, K. Yamada, and J. M. Bae, "Synthesis of organic/inorganic nanocomposites protonic conducting membrane through sol-gel processes," *Solid State Ionics*, vol. 118, no. 1-2, pp. 29–36, 1999.

[9] S. Ray and M. Okamoto, "Polymer/layered silicate nanocomposites: a review from preparation to processing," *Progress in Polymer Science*, vol. 28, p. 1539, 2003.

[10] R. Agrawal C and G. Pandey P, "Solid polymer electrolytes: materials designing and all-solid-state battery applications: an overview," *Journal of Physics D: Applied Physics*, vol. 41, Article ID 223001, 2008.

[11] P. Duangkaew and J. Woothikanokkhan, "Methanol permeability and proton conductivity of direct methanol fuel cell membranes based on sulfonated poly(vinyl alcohol)–layered silicate nanocomposites," *Journal of Applied Polymer Science*, vol. 109, p. 452, 2008.

[12] A. C. Finch, *Polyvinyl alcohol: properties and applications*, A. C. Finch, Ed., John Wiley Sons, Bristol, England, 1973.

[13] W. Wieczorek, Z. Florjanczyk, and J. R. Stevens, "Proton conducting polymer gels based on a polyacrylamide matrix," *Electrochimica Acta*, vol. 40, no. 13-14, pp. 2327–2330, 1995.

[14] S. Chandra, S. S. Sekhon, and N. Arora, "PMMA based protonic polymer gel electrolytes," *Ionics*, vol. 6, no. 1-2, pp. 112–118, 2000.

[15] S. Sekhon, "Conductivity behaviour of polymer gel electrolytes: Role of polymer," *Bulletin of Materials Science*, vol. 26, p. 321, 2003.

[16] S. Agrawal L and P. Shukla K, "Study of PTC effect in $BaTiO_3$ ceramics," *Journal of Pure & Applied Physics*, vol. 38, p. 611, 2000.

[17] J. Ramesh Babu, K. Ravindhranath, and K. Vijaya Kumar, "Structural and electrical properties of sodium citrate doped Poly(vinyl alcohol) Films for electrochemical cell applications," *Asian Journal of Chemistry*, vol. 29, no. 5, pp. 1049–1055, 2017.

[18] M. White, "Thin polymer films," *Thin Solid Films*, vol. 18, no. 2, pp. 157–172, 1973.

[19] J. B. Wagner and C. J. Wagner, "Electrical conductivity measurements on cuprous halides," *Chemical Reviews*, 1957.

[20] N. Chand, N. Rai, S. L. Agarwal, and S. K. PatelBull, "Neelesh Rai," *Journal of Materials Science*, vol. 34, no. 7, pp. 1297–1304, 2011.

[21] M. Hema, S. Selvasekerapandian, G. Hirankumar, A. Sakunthala, D. Arunkumar, and H. Nithya, "Structural and thermal studies of PVA:NH4I," *Journal of Physics and Chemistry of Solids*, vol. 70, no. 7, pp. 1098–1103, 2009.

[22] Z. Wen, T. Itoh, M. Ikeda, N. Hirata, M. Kubo, and O. Yamamoto, "Characterization of composite electrolytes based on a hyperbranched polymer," *Journal of Power Sources*, vol. 90, no. 1, pp. 20–26, 2000.

[23] H. Y. Sun, Y. Takeda, N. Imanishi, O. Yamamoto, and H.-J. Sohn, "Ferroelectric materials as a ceramic filler in solid composite polyethylene oxide-based electrolytes," *Journal of The Electrochemical Society*, vol. 147, no. 7, pp. 2462–2467, 2000.

[24] S. A. Hashmi, A. K. Thakur, and H. M. Upadhyaya, "Experimental studies on polyethylene oxide-NaClO4 based composite polymer electrolytes dispersed with Na2SiO3," *European Polymer Journal*, vol. 34, no. 9, pp. 1277–1282, 1998.

[25] P. S. Anantha and K. Hariharan, "Physical and ionic transport studies on poly(ethylene oxide)-NaNO 3 polymer electrolyte system," *Solid State Ionics*, vol. 176, no. 1-2, pp. 155–162, 2005.

[26] M. Watanabe, S. Nagano, K. Sanui, and N. Ogata, "Ion conduction mechanism in network polymers from poly(ethylene oxide) and poly(propylene oxide) containing lithium perchlorate," *Solid State Ionics*, vol. 18-19, no. 1, pp. 338–342, 1986.

[27] B. B. Owens, "Solid electrolyte batteries," *Advances in Electrochemistry and Electrochemical Engineering*, vol. 8, pp. 1–62, 1972.

[28] B. Owens, G. R. Argue, I. J. Groce, and L. D. Hermo, "Stability of the solid state cell Ag/Ag3SI/I2," *Journal of The Electrochemical Society*, vol. 116, no. 2, p. 312, 1969.

[29] S. S. Rao, K. V. S. Rao, M. Shareefuddin, U. V. S. Rao, and S. Chandra, "Ionic conductivity and battery characteristic studies on PEO+AgNO3 polymer electrolyte," *Solid State Ionics*, vol. 67, no. 3-4, pp. 331–334, 1994.

[30] S. Ramalingaiah, D. Srinivas Reddy, M. Jaipal Reddy, E. Laxminarsaiah, and U. V. Subba Rao, "Conductivity and discharge characteristic studies of novel polymer electrolyte based on PEO complexed with $Mg(NO_3)_2$ salt," *Materials Letters*, vol. 29, pp. 285–289, 1996.

[31] M. A. Ratner and D. F. Shriver, "ION transport in solvent-free polymers," *Chemical Reviews*, vol. 88, no. 1, pp. 109–124, 1988.

[32] P. B. Bhargav, V. M. Mohan, A. K. Sharma, and V. V. R. N. Rao, "Investigations on electrical properties of (PVA:NaF) polymer electrolytes for electrochemical cell applications," *Current Applied Physics*, vol. 9, no. 1, pp. 165–171, 2009.

[33] R. M. Hodge, G. H. Edward, and G. P. Simon, "Water absorption and states of water in semicrystalline poly(vinyl alcohol) films," *Polymer Journal*, vol. 37, no. 8, pp. 1371–1376, 1996.

[34] A. R. Reddy and R. Kumar, "Ionic conductivity and discharge characteristic studies of PVA-Mg(CH 3COO)2 solid polymer electrolytes," *International Journal of Polymeric Materials and Polymeric Biomaterials*, vol. 62, no. 2, pp. 76–80, 2013.

[35] S. S. Rao, M. J. Reddy, E. L. Narsaiah, and U. V. S. Rao, "Development of electrochemical cells based on (PEO + NaYF4) and (PEO + KYF4) polymer electrolytes," *Materials Science and Engineering: B Advanced Functional Solid-State Materials*, vol. 33, no. 2-3, pp. 173–177, 1995.

[36] V. S. Reddy, A. K. Sharma, and V. V. R. N. Rao, "Effect of plasticizer on electrical conductivity and cell parameters of PVP + PVA + $KClO_3$ blend polymer electrolyte system," *Journal of Power Sources*, vol. 111, 375 pages, 2002.